Journal of Catalysis 260 (2008) 262–269

Contents lists available at ScienceDirect

Journal of Catalysis

www.elsevier.com/locate/jcat

Hydrodesulfurization properties of cobalt–nickel phosphide catalysts: Ni-rich materials are highly active

Autumn W. Burns, Amy F. Gaudette, Mark E. Bussell *

Department of Chemistry, MS-9150, Western Washington University, 516 High Street, Bellingham, WA 98225, USA

ARTICLE INFO

Article history:
Received 30 July 2008
Revised 30 September 2008
Accepted 2 October 2008
Available online 31 October 2008

Keywords:
Hydrodesulfurization
HDS
Nickel phosphide
Cobalt phosphide
Bimetallic phosphide
Cobalt–nickel phosphide

ABSTRACT

The HDS properties of a series of $Co_xNi_{2-x}P_y/SiO_2$ catalysts have been investigated as a function of the Co/Ni molar ratio (for a fixed P/Me molar ratio) and of the P/Me molar ratio (for a fixed Co/Ni molar ratio). An oxidic precursor composition of $Co_{0.08}Ni_{1.92}P_{2.00}$ on the silica support yielded the bimetallic phosphide phase having the highest HDS activity, 34% higher than that of an optimized nickel phosphide catalyst prepared from an oxidic precursor having a composition of $Ni_{2.00}P_{1.60}$. X-ray photoelectron spectroscopy revealed Ni-rich $Co_xNi_{2-x}P_y/SiO_2$ catalysts to have surface enrichment of P (relative to $Ni_{2.00}P_{1.60}/SiO_2$ and $Co_{2.00}P_{1.00}/SiO_2$ catalysts) and to incorporate remarkably low amounts of S during HDS testing. The high activity of these $Co_xNi_{2-x}P_y/SiO_2$ catalysts is attributed to surface enrichment of P relative to nickel phosphide, which results in improved resistance to S incorporation under HDS conditions. Consistent with these findings and the solid-state chemistry evidence that suggests that Ni atoms in Ni-rich $Co_xNi_{2-x}P_y/SiO_2$ catalysts occupy disproportionately more pyramidal M(2) sites than tetrahedral M(1) sites, we conclude that the high site densities of these catalysts are due to Ni atoms in surface M(2) sites, which results in P-enriched surfaces that are resistant to site blockage due to S incorporation.

1. Introduction

Responding to expectations that lower quality crude oil feedstocks containing high sulfur and nitrogen levels will be increasingly processed for the production of ultralow sulfur transportation fuels in the future, a few laboratories are exploring the possibility of using highly active transition metal phosphides as the active phase for a new generation of hydrotreating catalysts. A number of monometallic phosphide phases (e.g., MoP [1–6], WP [3,7,8], CoP [9–11], Co_2P [11–15] and Ni_2P [9,10,12,14,16–29]) have been a focus of recent research efforts within the hydrotreating catalysis community, as have a smaller number of bimetallic phosphides (e.g., NiMoP [3,15,19], Ni_xMoP [28,30], Ni_xMo_yP [31], CoMoP [3,15], Co_xMoP [32], Co_xNi_2P [28,32]). While one might expect to observe a synergistic effect between two metals in bimetallic phosphides similar to that observed for sulfided Ni–Mo catalysts; the catalytic activities exhibited by some bimetallic phosphides suggest more complex behavior. Bimetallic phosphide phases have been reported to have lower (e.g., NiMoP [19]), intermediate (e.g., Ni_xMo_yP [31]) or higher (e.g., Co_xNi_2P [28,32]) catalytic activities than monometallic phosphides of the same metals for hydrodesulfurization (HDS) or hydrodenitrogenation (HDN) processing. In addition to the influence of the metal(s) in the phosphide phase on catalytic activity, investigations of the properties of metal phosphides have also revealed that HDS or HDN activities can vary substantially with the phosphorus-to-metal (P/Me) molar ratio of the supported phosphides for Ni_xP_y/SiO_2 [17,24,27] and Co_xP_y/SiO_2 [11] catalysts.

A number of bimetallic phosphides of interest for hydrotreating catalysis form solid solutions (e.g., $Mo_xNi_{2-x}P$ [33], $Co_xNi_{2-x}P$ [34]) in which the metal ratio can be changed while maintaining the crystal structure of the material. As a consequence, the effect of the metal composition on the catalytic properties of such bimetallic phosphide phases can be carefully probed, and optimal compositions determined. In this study, the HDS properties of a series of $Co_xNi_{2-x}P_y/SiO_2$ catalysts have been investigated as a function of the Co/Ni molar ratio (for a fixed P/Me molar ratio) and of the P/Me molar ratio (for a fixed Co/Ni molar ratio). An oxidic precursor composition of $Co_{0.08}Ni_{1.92}P_{2.00}$ on the silica support yielded the bimetallic phosphide phase having the highest HDS activity, 34% higher than that of an optimized nickel phosphide catalyst prepared from an oxidic precursor having a composition of $Ni_{2.00}P_{1.60}$. The high activity of this $Co_xNi_{2-x}P_y/SiO_2$ catalyst is attributed to surface enrichment of P relative to nickel phosphide, which results in improved resistance to S incorporation under HDS conditions.

* Corresponding author. Fax: +1 360 650 2826.
E-mail address: Mark.Bussell@wwu.edu (M.E. Bussell).

0021-9517/$ – see front matter
doi:10.1016/j.jcat.2008.10.001

2. Experimental methods

2.1. Catalyst synthesis

Oxidic precursors of $Co_xNi_{2-x}P_y/SiO_2$ catalysts (with metal loadings equivalent to 25 wt% Me_2P, Me = Co + Ni) were prepared as follows. Prior to use, the silica (SiO_2, Cab-O-Sil, M-7D grade, 200 m^2/g) was calcined in air at 773 K for 3 h. The silica support was then impregnated with an aqueous solution containing selected amounts of $Co(NO_3)_2{\cdot}6H_2O$ (Alfa Aesar, 99.9985%) and $Ni(NO_3)_2{\cdot}6H_2O$ (Alfa Aesar, 99.9985%) followed by drying at 383 K. The dried material was subsequently impregnated with $NH_4H_2PO_4$ (Baker, 99.1%), followed by drying at 383 K, and calcination at 773 K for 3 h. As an example, the oxidic precursor of a $Co_{1.00}Ni_{1.00}P_{1.00}/SiO_2$ catalyst was prepared by impregnating 2.50 g of freshly calcined SiO_2 with an aqueous solution of 1.632 g of $Co(NO_3)_2{\cdot}6H_2O$ and 1.631 g of $Ni(NO_3)_2{\cdot}6H_2O$, and then with an aqueous solution of 0.741 g of $NH_4H_2PO_4$. Following drying and calcination, a portion of the oxidic precursor was subjected to a temperature-programmed reduction (TPR) procedure in which the precursor was first degassed in a 60 mL/min flow of He (Airgas, 99.999%), then reduced in a 300 mL/min of H_2 (Airgas, 99.999%) while the temperature was increased from room temperature to 923 K at a rate of 1 K/min. Following the reduction process, the samples were cooled to room temperature in a continued flow of H_2 (300 mL/min) and then flushed with He (60 mL/min) for 15 min. The samples were then passivated in a 1.0 mol% O_2/He (Airgas 99%) mixture (30 mL/min) for 3 h at room temperature. The details of the TPR procedure have been described elsewhere [20]. In addition to varying the metal composition of the oxidic precursors of $Co_xNi_{2-x}P_{1.00}/SiO_2$ catalysts over the range $0 \leqslant x \leqslant 2.00$, the P/Me molar ratio was also varied for oxidic precursors having compositions of $Co_{0.08}Ni_{1.92}P_y/SiO_2$, where $1.00 \leqslant y \leqslant 2.20$. For the monometallic phosphide catalysts, the oxidic precursor compositions were $Co_{2.00}P_{1.00}/SiO_2$ and $Ni_{2.00}P_{1.60}/SiO_2$.

2.2. Catalyst characterization

2.2.1. Bulk characterization measurements

X-ray diffraction (XRD) patterns of the $Co_xNi_{2-x}P_{1y}/SiO_2$ catalysts were obtained using a PANalytical X'Pert Pro diffractometer equipped with a monochromatic CuK_α source ($\lambda = 1.54050$ Å). Transmission electron microscopy (TEM) measurements were obtained with a JEOL 2010 high resolution transmission electron microscope operating at 200 keV. The samples were placed on a 200 mesh copper grid coated with formvar and carbon. Analysis of the Co, Ni and P contents of $Co_xNi_{2-x}P_y/SiO_2$ catalysts was carried out by Huffman Laboratories, Inc.

2.2.2. Surface characterization measurements

X-ray photoelectron spectroscopy (XPS) measurements were carried out using a Physical Electronics Quantum 2000 Scanning ESCA Microprobe system with a focused monochromatic AlK_α X-ray (1486.7 eV) source and a spherical section analyzer. The spectra were collected with a pass energy of 23.5 eV. The spectra were referenced to an energy scale with binding energies for Cu($2p_{3/2}$) at 932.67 ± 0.05 eV and Au(4f) 84.0 ± 0.05 eV. Binding energies were corrected for sample charging using the C(1s) peak at 284.6 eV for adventitious carbon as a reference. Low energy electrons and argon ions were used for specimen neutralization. The XPS spectra were acquired for $Co_xNi_{2-x}P_y/SiO_2$ catalysts following passivation and transfer through air to the spectrometer. XPS spectra were also acquired for a few $Co_xNi_{2-x}P_y/SiO_2$ catalysts after HDS testing for 48–60 h. In these cases, the tested catalysts were cooled from the reaction temperature to room temperature in flowing He (60 mL/min) and then passivated in a flowing 1.0 mol% O_2/He mixture (30 mL/min) for 2 h at room temperature. The catalysts were then transferred through air to the XPS spectrometer.

BET surface area measurements were acquired using a Micromeritics PulseChemisorb 2700 instrument. 0.1000 g of catalyst was placed in a quartz U-tube and degassed at room temperature in a 60 mL/min flow He for 30 min. The sample was treated in a flow of He (45 mL/min) for 2 h at 623 K and then cooled to room temperature in a continued He flow. The BET measurements were carried out as described elsewhere [20].

Oxygen (O_2) pulsed chemisorption measurements were also obtained using the Micromeritics PulseChemisorb 2700 instrument. 0.1000 g of catalyst was degassed in 60 mL/min He at room temperature for 30 min. Prior to the measurements, the samples were either reduced or sulfided in-situ. For reduction, samples were heated from room temperature to 650 K in a 60 mL/min flow of H_2 and held at this temperature for 2 h. For sulfidation, samples were heated from room temperature to 650 K in a 60 mL/min flow of a 3.0 mol% H_2S/H_2 mixture, held at this temperature for 2 h, and then reduced in a 60 mL/min flow of H_2 at 623 K for 1 h. All of the samples were then degassed in 45 mL/min He at 673 K for 1 h. The O_2 chemisorption capacity measurements were carried out at 196 K using a procedure described elsewhere [20]. A 10.3 mol% O_2/He mixture (Airco) was used to obtain the O_2 chemisorption capacity measurements.

2.2.3. Thiophene HDS activity measurements

Thiophene HDS activity measurements were carried out using an atmospheric pressure flow reactor according to a method described previously [20,22]. All catalysts were degassed in He (60 mL/min) at room temperature for 30 min. The sample was then heated to the reaction temperature of 643 K and the flow was switched to a 3.2 mol% thiophene/H_2 reactor feed (50 mL/min). The gas effluent was sampled at 1 h intervals and the final measurement was taken after 48 h on-stream. The total product peak areas from the chromatogram were used to calculate the thiophene HDS activities ($nmol_{Th}/g_{cat}\,s$) for the catalysts.

3. Results

3.1. Characterization of as-prepared catalysts

The nominal and actual compositions of the as-prepared $Co_xNi_{2-x}P_y/SiO_2$ catalysts (for which bulk elemental analyses were carried out) are listed in Table 1. In cases where P/Me > 0.5 for the oxidic precursors, it is not surprising that the actual compositions of the metal phosphide phases contain less P than the nominal compositions, as some excess P has been shown to be lost from oxidic precursors of Co_xP_y/SiO_2 and Ni_xP_y/SiO_2 catalysts during TPR [11,24]. All of the catalysts are somewhat P-rich ($0.53 \leqslant$ P/Me $\leqslant 0.61$) compared to the expected stoichiometry of P/Me = 0.50. X-ray diffraction patterns for $Co_xNi_{2-x}P_{1.00}/SiO_2$ catalysts with a range of metal compositions are shown in Fig. 1. Catalysts with nominal compositions of $Co_{2.00}P_{1.00}/SiO_2$ and $Co_{1.75}Ni_{0.25}P_{1.00}/SiO_2$ exhibit XRD patterns similar to that of a JCPDS reference pattern for Co_2P (card no. 32-0306 [35]). For $Co_xNi_{2-x}P_{1.00}/SiO_2$ catalysts with $x \leqslant 1.50$ (i.e. starting with $Co_{1.50}Ni_{0.50}P/SiO_2$ in Fig. 1), the XRD patterns for the bimetallic phosphide phases are consistent with a JCPDS reference pattern for Ni_2P (card no. 089-2742 [35]). While not shown, XRD patterns for $Co_{0.08}Ni_{1.92}P_y/SiO_2$ catalysts, for which an excess of P was used in the oxidic precursors ($1.2 \leqslant y \leqslant 2.2$), are similar to the reference pattern for Ni_2P shown in Fig. 1. Based on calculations using the Scherrer equation, the $Co_xNi_{2-x}P_y/SiO_2$ catalysts in this study had crystallite sizes in the range 33–48 nm with an average of 42 nm.

Table 1
Bulk and surface compositions of selected $Co_xNi_{2-x}P/SiO_2$ catalysts.

Nominal composition	Actual composition	Surface composition	Surface composition (post HDS)
$Co_{2.00}P_{1.00}$	$Co_{1.88}P_{1.00}$	$Co_{3.46}P_{1.00}$	$Co_{5.42}P_{1.00}S_{0.67}$
$Co_{1.50}Ni_{0.50}P_{1.00}$	$Co_{1.33}Ni_{0.46}P_{1.00}$	$Co_{1.02}Ni_{0.29}P_{1.00}$	–
$Co_{1.00}Ni_{1.00}P_{1.00}$	$Co_{0.90}Ni_{0.91}P_{1.00}$	$Co_{0.47}Ni_{1.18}P_{1.00}$	$Co_{1.13}Ni_{1.77}P_{1.00}S_{0.30}$
$Co_{0.50}Ni_{1.50}P_{1.00}$	$Co_{0.45}Ni_{1.33}P_{1.00}$	$Co_{0.24}Ni_{1.03}P_{1.00}$	–
$Co_{0.25}Ni_{1.75}P_{1.00}$	$Co_{0.23}Ni_{1.60}P_{1.00}$	$Co_{0.28}Ni_{1.51}P_{1.00}$	–
$Co_{0.13}Ni_{1.87}P_{1.00}$	$Co_{0.11}Ni_{1.72}P_{1.00}$	$Co_{0.20}Ni_{1.63}P_{1.00}$	–
$Co_{0.08}Ni_{1.92}P_{1.00}$	$Co_{0.07}Ni_{1.77}P_{1.00}$	$Co_{0.24}Ni_{0.1.46}P_{1.00}$	$Co_{0.15}Ni_{1.49}P_{1.00}S_{0.09}$
$Co_{0.08}Ni_{1.92}P_{1.60}$	$Co_{0.06}Ni_{1.50}P_{1.00}$	$Co_{0.09}Ni_{1.01}P_{1.00}$	$Co_{0.13}Ni_{1.59}P_{1.00}S_{0.06}$
$Co_{0.04}Ni_{1.96}P_{1.00}$	$Co_{0.04}Ni_{1.80}P_{1.00}$	$Co_{0.17}Ni_{1.78}P_{1.00}$	–
$Ni_{2.00}P_{1.60}$	$Ni_{1.64}P_{1.00}$	$Ni_{2.23}P_{1.00}$	$Ni_{2.87}P_{1.00}S_{0.32}$

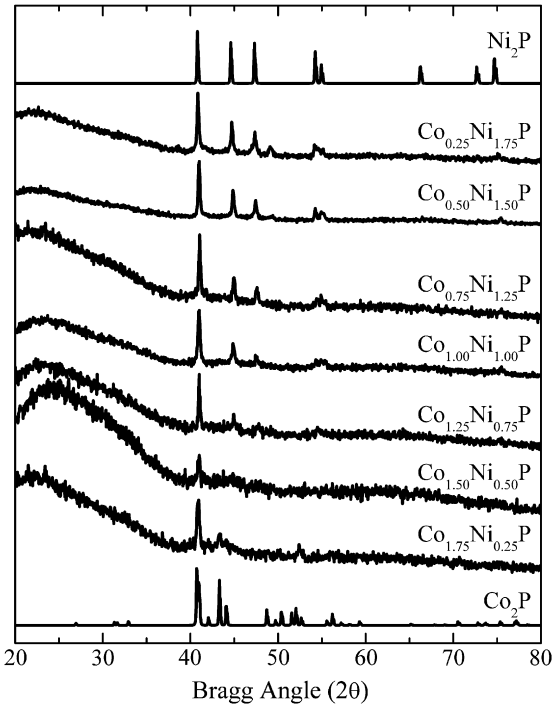

Fig. 1. XRD patterns for $Co_xNi_{2-x}P_{1.00}/SiO_2$ catalysts having different metal ratios.

Low- and high-resolution TEM images of a $Co_{0.13}Ni_{1.87}P_{1.00}/SiO_2$ catalyst are shown in Fig. 2. The low-resolution image reveals globularly shaped particles on the silica support having a range of sizes. The high-resolution TEM image shows a $Co_{0.13}Ni_{1.87}P_{1.00}$ particle on the silica support having a diameter of approximately 14 nm; the measured spacing between lattice fringes of 5.1 Å is consistent with the *d*-spacing of the (100) crystallographic plane of Ni_2P (card no. 089-2742 [35]). TEM images were acquired for some of the other $Co_xNi_{2-x}P_y/SiO_2$ catalysts as well and these revealed similar dispersions and particle sizes.

Shown in Fig. 3 are XPS spectra in the Ni($2p_{3/2}$), Co($2p_{3/2}$) and P($2p_{3/2}$) regions for $Co_{1.75}Ni_{0.25}P_{1.00}/SiO_2$, $Co_{1.00}Ni_{1.00}P_{1.00}/SiO_2$ and $Co_{0.25}Ni_{1.75}P_{1.00}/SiO_2$ catalysts. The XPS spectra for these catalysts exhibit no unexpected features relative to those reported previously from our laboratory for Co_2P/SiO_2 [11] and Ni_2P/SiO_2 [20,24] catalysts. Since the $Co_xNi_{2-x}P_y/SiO_2$ catalysts were passivated in a 1 mol% O_2/He mixture following TPR synthesis, the XPS spectra in Ni($2p_{3/2}$), Co($2p_{3/2}$) and P($2p_{3/2}$) regions show peaks for oxidized species as well as for underlying reduced species associated with the phosphide phases. The binding energies for the oxidized Ni (855.2–856.4 eV), Co (781.2–781.6 eV) and P (132.8–133.6 eV) are consistent with assignments by others to Ni^{2+}, Co^{2+} and P^{5+} species, respectively [14]. The binding energies for peaks associated with reduced Ni (852.0–853.0 eV) and Co (777.4–778.2 eV) species are consistent with those reported for zero-valent Ni (852.5–852.9 eV [36]) and Co (778.1–778.2 eV [36]). In contrast, the binding energies for reduced P species (128.6–129.6 eV) are below that of elemental phosphorus (130.2 eV [36]), which suggests somewhat increased electron density for P in the $Co_xNi_{2-x}P_y$ phase. Our laboratory and others have observed similar shifts of the P($2p_{3/2}$) binding energy for bulk and supported Co_2P [11,14,37,38] and Ni_2P [14,20,24,37] catalysts, and concluded that a slight transfer of electron density from the metal to P occurs in these phosphides. In these cases, however, the metal (Co, Ni) $2p_{3/2}$ binding energy was measured to be somewhat higher than those of the zero-valent metals, which is not what was observed for the $Co_{1.75}Ni_{0.25}P_{1.00}/SiO_2$, $Co_{1.00}Ni_{1.00}P_{1.00}/SiO_2$ and $Co_{0.25}Ni_{1.75}P_{1.00}/SiO_2$ catalysts. Abu and

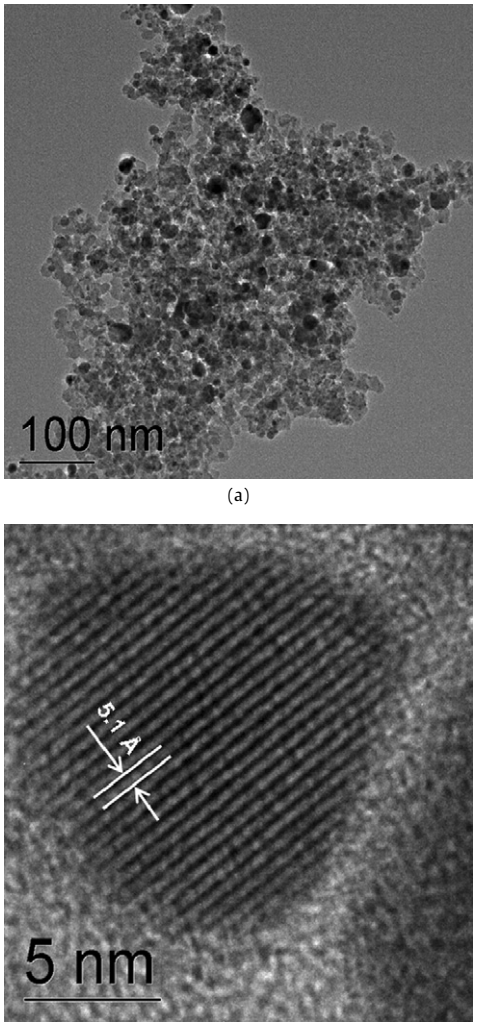

Fig. 2. (a) Low and (b) high resolution images of a $Co_{0.13}Ni_{1.87}P_{1.00}/SiO_2$ catalyst.

Table 2
Catalytic data for selected $Co_xNi_{2-x}P/SiO_2$ catalysts.

Nominal composition	BET surface area (m^2/g)	Chemisorption capacity ($\mu mol_{O_2}/g$)		HDS activity[a] ($nmol_{Th}/(g\,s)$)
		H_2 pretreatment	H_2/H_2S pretreatment	
$Co_{2.00}P_{1.00}$	96	70	4	183
$Co_{1.50}Ni_{0.50}P_{1.00}$	99	69	7	61
$Co_{1.00}Ni_{1.00}P_{1.00}$	99	73	23	281
$Co_{0.50}Ni_{1.50}P_{1.00}$	94	55	99	449
$Co_{0.25}Ni_{1.75}P_{1.00}$	100	87	97	1082
$Co_{0.13}Ni_{1.87}P_{1.00}$	101	111	119	1701
$Co_{0.08}Ni_{1.92}P_{1.00}$	99	127	163	2020
$Co_{0.08}Ni_{1.92}P_{1.60}$	99	118	160	3045
$Co_{0.04}Ni_{1.96}P_{1.00}$	97	156	149	2545
$Ni_{2.00}P_{1.60}$	81	153	135	2283

[a] Thiophene HDS activity after 48 h on-stream.

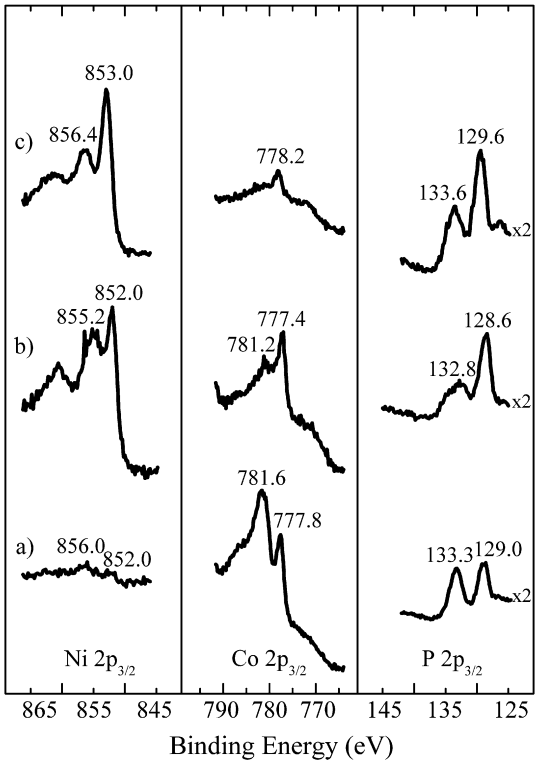

Fig. 3. XPS spectra of (a) $Co_{1.75}Ni_{0.25}P_{1.00}/SiO_2$, (b) $Co_{1.00}Ni_{1.00}P_{1.00}/SiO_2$ and (c) $Co_{0.25}Ni_{1.75}P_{1.00}/SiO_2$ catalysts.

Smith [32] reported XPS spectra for unsupported Co_xNi_2P materials for which $0.08 \leqslant x \leqslant 0.34$. These authors measured a relatively low Ni($2p_{3/2}$) binding energy of 852.7 eV for $Co_{0.34}Ni_2P$, which is consistent with the binding energy of 852.0 eV measured in this study for $Co_{1.75}Ni_{0.25}P_{1.00}/SiO_2$ and $Co_{1.00}Ni_{1.00}P_{1.00}/SiO_2$ catalysts. These authors attributed the low Ni($2p_{3/2}$) binding energy to the presence of $Ni_{12}P_5$ in $Co_{0.34}Ni_2P$ (as determined by XRD). Our laboratory had previously reported a lower Ni($2p_{3/2}$) binding energy for a $Ni_{12}P_5/SiO_2$ catalyst (853.0 eV) compared to a Ni_2P/SiO_2 catalyst (853.5 eV).

Surface compositions determined from the XPS spectra in Fig. 3 as well as those for other $Co_xNi_{2-x}P_y/SiO_2$ catalysts are listed in Table 1. The monometallic phosphide catalysts $Co_{2.00}P_{1.00}/SiO_2$ and $Ni_{2.00}P_{1.60}/SiO_2$, which correspond to phase-pure Co_2P and Ni_2P on the silica support, respectively, both have metal-rich surface compositions relative to the measured bulk compositions. The $Ni_{2.00}P_{1.60}/SiO_2$ catalyst, for example, had a surface molar ratio of $P^s/Ni^s = 0.45$ and a bulk molar ratio of $P/Ni = 0.61$. The bimetallic phosphide catalysts, on the other hand, have P-rich surfaces compared to the bulk compositions. As an example, surface and bulk molar ratios of $P^s/Me^s = 0.91$ and $P/Me = 0.64$, respectively, were observed for the $Co_{0.08}Ni_{1.92}P_{1.60}/SiO_2$ catalyst, where Me = Co + Ni. Abu and Smith [32] reported surface, but not bulk compositions for unsupported Co_xNi_2P and Ni_2P materials. Unsupported Co_xNi_2P catalysts with $0.08 \leqslant x \leqslant 0.34$ had surface molar ratios of $P^s/Me^s = 1.2$–4.8, while unsupported Ni_2P had $P^s/Ni^s = 0.5$.

The BET surface areas and oxygen (O_2) chemisorption capacities of the $Co_xNi_{2-x}P_y/SiO_2$ catalysts are listed in Table 2. The surface areas of the catalysts were similar, while the O_2 chemisorption capacities measured following H_2 or H_2S/H_2 pretreatments varied dramatically depending on the metal composition of the phosphide catalysts. For the H_2 pretreatment, the chemisorption capacities followed an increasing trend as the amount of Ni in the $Co_xNi_{2-x}P_y/SiO_2$ catalysts increases. For the H_2S/H_2 pretreatment, a similar trend was observed except that a maximum in the O_2 chemisorption capacity was achieved at $x = 0.08$, with about a 20% decrease observed as x approached 0 (i.e. $Ni_{2.00}P_{1.60}/SiO_2$). For catalysts with high Co contents, the O_2 chemisorption capacities following H_2S/H_2 pretreatment were significantly smaller than following a H_2 pretreatment, while for catalysts with high Ni contents the chemisorption capacities following the two pretreatments were similar or slightly higher for the H_2S/H_2 pretreatment. In a recent study, we reported that for Co_xP_y/SiO_2 catalysts having $0.50 \leqslant P/Co \leqslant 2.00$, all catalysts in this series adsorbed dramatically more O_2 following H_2 pretreatment than after H_2S/H_2 pretreatment [11].

3.2. Thiophene HDS activities

The HDS activities of the $Co_xNi_{2-x}P_y/SiO_2$ catalysts as a function of time on-stream exhibit similar trends to those reported previously for Ni_2P/SiO_2 [20] and Co_2P/SiO_2 [11] catalysts. The activities were remarkably stable from time zero to over 75 h, when a measurement was typically stopped. There was no evidence for deactivation of $Co_xNi_{2-x}P_y/SiO_2$ catalysts during the early stages of the testing period, or at least on the timescale of the effluent sampling (15 min intervals) from which catalyst activities were calculated. The HDS activities of the $Co_xNi_{2-x}P_y/SiO_2$ catalysts (after 48 h on-stream) are plotted as a function of the Ni metal fraction (Ni/(Ni + Co)) in Fig. 4 and are listed for some of the catalysts in Table 2. Starting from the Co-rich end of the plot, the HDS activities are quite low from $Co_{2.00}P_{1.00}/SiO_2$ up through $Co_{0.50}Ni_{1.50}P_{1.00}/SiO_2$, but the activities climb steadily as the catalysts become increasingly Ni-rich. As indicated by the activity data plotted in Fig. 4, catalysts of composition $Co_xNi_{2-x}P_{1.00}/SiO_2$, where $0.04 \leqslant x \leqslant 0.08$, had activities similar to that of a $Ni_{2.00}P_{1.60}/SiO_2$ catalyst. This nickel phosphide catalyst had been previously optimized by adjusting the P/Ni molar ratio of its oxidic precursor to be 0.80 [24]. To explore the effect of the metal-to-phosphorus molar ratio on HDS activity, $Co_xNi_{2-x}P_y/SiO_2$ catalysts with a fixed metal composition corre-

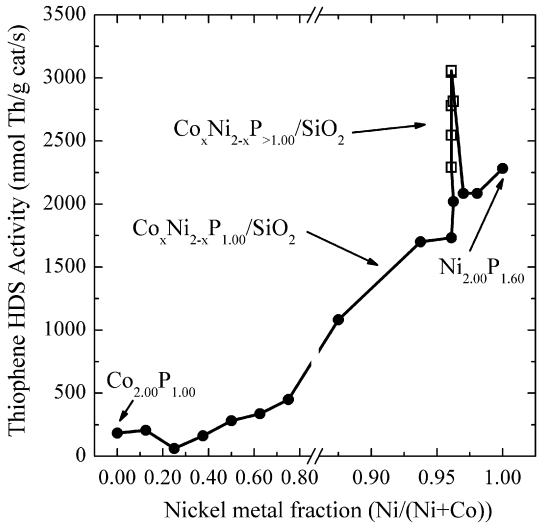

Fig. 4. Thiophene HDS activity versus nominal Ni metal fraction for $Co_xNi_{2-x}P_y/SiO_2$ catalysts.

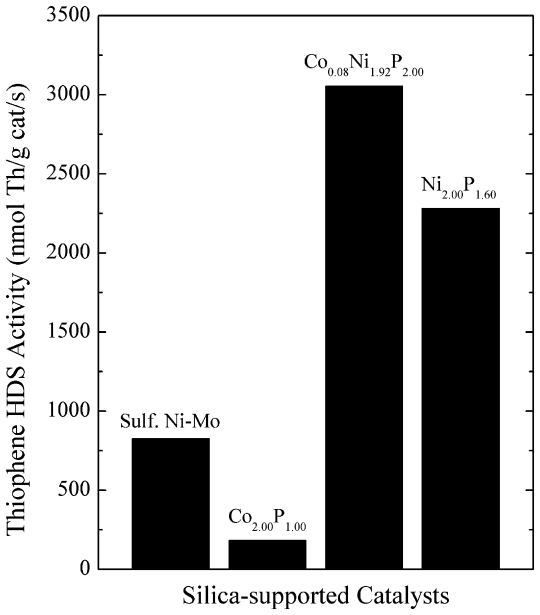

Fig. 5. Comparison of thiophene HDS activities for sulfided Ni–Mo/SiO_2, $Co_{2.00}P_{1.00}/SiO_2$, $Ni_{2.00}P_{1.60}/SiO_2$ and $Co_{0.08}Ni_{1.92}P_{2.00}/SiO_2$ catalysts.

sponding to $x = 0.08$ (i.e. $Co_{0.08}Ni_{1.92}P_y/SiO_2$) were prepared with different P contents in the oxidic precursors ($1.00 \leqslant y \leqslant 2.20$). The HDS activities of these catalysts are also plotted in Fig. 4 (open square symbols for catalysts with P/Me > 0.50). The catalyst with the optimal composition, $Co_{0.08}Ni_{1.92}P_{2.00}/SiO_2$ (P/Me = 1.00) had an HDS activity that was 34% higher than that of a $Ni_{2.00}P_{1.60}/SiO_2$ catalyst. The HDS activities after 48 h on-stream for the most active $Co_xNi_{2-x}P_y/SiO_2$ catalyst investigated, $Co_{0.08}Ni_{1.92}P_{2.00}/SiO_2$, along with those for the monometallic phosphide catalysts, $Co_{2.00}P_{1.00}/SiO_2$ and $Ni_{2.00}P_{1.60}/SiO_2$, and for a sulfided Ni–Mo/SiO_2 catalyst reported previously [20] are compared in Fig. 5. In addition to being substantially more active than the monometallic phosphide catalysts, the $Co_{0.08}Ni_{1.92}P_{2.00}/SiO_2$ catalyst is over 3.5 times more active than the sulfided Ni–Mo/SiO_2 catalyst (7.9 wt% NiO, 30.4 wt% MoO_3) [20]. Consistent with our measurements, Abu et al. [32] observed an unsupported $Co_{0.08}Ni_2P$ catalyst (P/Me = 0.48) to have an activity 67% higher than that of a Ni_2P catalyst (P/Ni = 0.50) for HDS of 4,6-DMDBT. It is worth noting that these authors did not use an excess of P in the oxidic precursors of their catalysts (indeed less than a stoichiometric amount of P in the $Co_{0.08}Ni_2P$ catalyst).

3.3. Characterization of HDS-tested catalysts

XRD patterns and XPS spectra were acquired for a few $Co_xNi_{2-x}P_y/SiO_2$ catalysts after 48 h of HDS testing and the surface compositions for these catalysts are listed in Table 1. XRD patterns of the tested catalysts showed no evidence for the decomposition of the phosphide phases or for the formation of new crystalline phases during HDS. Plotted in Fig. 6 are the surface sulfur-to-metal molar ratios (S^s/Me^s) of these *tested* catalysts as a function of the surface metal-to-phosphorus (P^s/Me^s) ratio of the *as-prepared* catalysts. A trend is apparent in which the surface S content of the tested catalysts decreased substantially as the surface P content of the as-prepared catalysts increased. The most active of these catalysts, $Co_{0.08}Ni_{1.92}P_{1.60}/SiO_2$, had the most P-enriched surface and had a S/Me molar ratio that was just 31% of that of the $Ni_{2.00}P_{1.60}/SiO_2$ catalyst. Abu and Smith measured a substantially higher S content for a $Co_{0.4}Ni_2P/Al_2O_3$ catalyst [28], but this is not surprising given that this catalyst had a higher Co content and a lower P content (P/Me = 0.46) than the $Co_{0.08}Ni_{1.92}P_y/SiO_2$ catalysts investigated in the current study. In our work, a $Co_{1.00}Ni_{1.00}P_{1.00}/SiO_2$ catalyst incorporated twice as much S than did a $Co_{0.08}Ni_{1.92}P_{1.00}/SiO_2$ catalyst (on an S/Me basis), and an earlier study revealed a $Ni_{12}P_5/SiO_2$ catalyst (P/Ni = 0.41) incorporated significantly more sulfur than did a Ni_2P/SiO_2 catalyst (P/Ni = 0.61) [24].

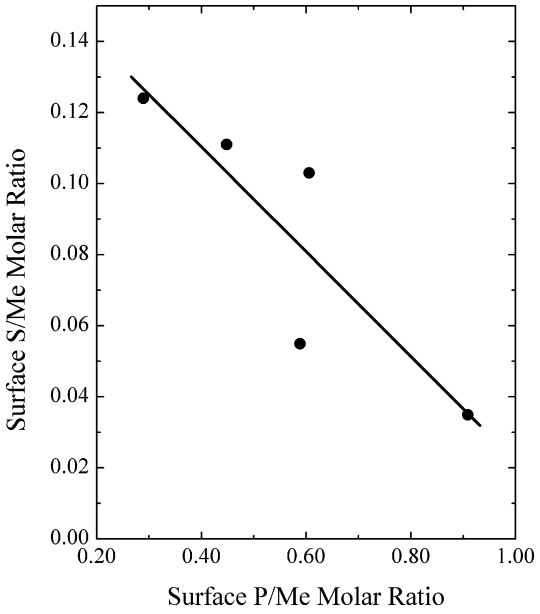

Fig. 6. Surface S/Me molar ratio of HDS-tested $Co_xNi_{2-x}P_y/SiO_2$ catalysts plotted versus the surface P/Me molar ratio of the as-prepared catalysts.

4. Discussion

4.1. Solid-state and surface chemistry of $Co_xNi_{2-x}P_y/SiO_2$ catalysts

The monometallic phosphides Co_2P and Ni_2P adopt orthorhombic (Pnma space group [39]) and hexagonal ($P\bar{6}2m$ space group [39]) structures, respectively. Both structure types contain two kinds of metal sites, one in which the metal atom is surrounded by four P atoms in a tetrahedral geometry (M(1) sites), and a second in which the metal atom is surrounded by five P atoms in a square pyramidal geometry (M(2) sites) [40]. The orthorhombic and hexagonal structures differ in the packing of rhombohedral

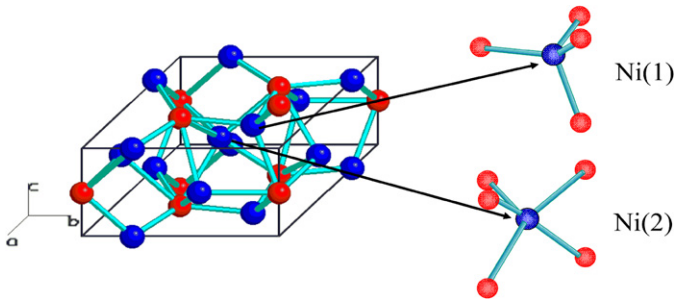

Fig. 7. Ni_2P structure showing the tetrahedral Ni(1) and pyramidal Ni(2) sites.

subunits containing M(1) and M(2) sites within the crystals [40]. The two kinds of sites are shown for Ni_2P in Fig. 7. Bimetallic phosphides having the general formula $Co_xNi_{2-x}P$ exhibit hexagonal structures similar to that of Ni_2P over the compositional range for which $0 \leqslant x \leqslant 1.7$, while the more Co-rich materials corresponding to $x > 1.7$ adopt the orthorhombic structure associated with Co_2P [40]. The XRD patterns for the $Co_xNi_{2-x}P_y/SiO_2$ catalysts in this study (Fig. 1) are consistent with these findings, with only the $Co_{1.75}Ni_{0.25}P_{1.00}/SiO_2$ catalyst exhibiting peaks consistent with the Co_2P structure. Neutron diffraction measurements revealed that there is ordering of the metals in the M(1) and M(2) sites in $Co_xNi_{2-x}P$ materials [41,42], as have Mössbauer spectroscopy measurements for the related $Fe_xNi_{2-x}P$ materials [43]. For the most Ni-rich $Co_xNi_{2-x}P$ material investigated via neutron diffraction, $Co_{0.8}Ni_{1.2}P$, Artigas et al. [42] observed that 89% of the M(2) sites were occupied by Ni atoms while just 31% of the M(1) sites were occupied by Ni atoms, and the extent of ordering among the two sites increased with increasing Ni content. Consistent with the observations for $Co_xNi_{2-x}P$ materials, the extent of ordering among M(1) and M(2) sites in $Fe_xNi_{2-x}P$ materials was found to depend on the metal composition of these materials, which adopt the hexagonal structure over the full range of compositions ($0 \leqslant x \leqslant 2$). Ni atoms preferentially occupy M(1) sites for Fe-rich materials ($1.7 \leqslant x \leqslant 2.0$) and M(2) sites for Ni-rich materials ($0 \leqslant x < 1.7$) [43]. For the most Ni-rich $Fe_xNi_{2-x}P$ material investigated, $Fe_{0.20}Ni_{1.80}P$, the Fe atoms occupy exclusively M(1) sites, resulting in a substantial excess of Ni atoms in M(2) sites [43]. Mössbauer spectral data obtained in our laboratory for $Fe_xNi_{2-x}P/SiO_2$ catalysts are consistent with those for the bulk $Fe_xNi_{2-x}P$ system [44]. With these solid-state chemistry findings in mind, we conclude that Ni atoms in the $Co_xNi_{2-x}P_y/SiO_2$ catalysts investigated in the current study occupy disproportionately more pyramidal M(2) sites than tetrahedral M(1) sites.

Oyama et al. [45] recently reported that the distribution of Ni in M(1) and M(2) sites of supported Ni_2P particles is sensitive to the size of the phosphide particles. As the Ni_2P crystallite size (as calculated using the Scherrer equation) decreased from 10.1 to 3.8 nm, the proportion of Ni in M(2) sites increased relative to Ni in M(1) sites. Significantly, the bulk P/Ni molar ratio and the activity of the Ni_2P catalysts for HDS of 4,6-DMDBT was observed to correlate with the proportion of Ni in M(2) sites. The authors concluded that the surfaces of the Ni_2P particles terminate with M(2) sites and, therefore, the proportion of these sites in the particles increases as the particle size decreases. As the proportion of Ni in M(2) sites increases, the bulk P/Ni molar ratio also increases as square pyramidal Ni atoms (M(2)) are surrounded by five P atoms while tetrahedral Ni atoms (M(1)) are surrounded by four P atoms. Finally, the authors concluded that the active sites for HDS of 4,6-DMDBT are Ni atoms in surface M(2) sites as the HDS activity increases with the increasing proportion of Ni in M(2) sites. This conclusion is consistent with the surfaces of the supported Ni_2P particles being terminated with M(2) sites as discussed above.

Studies in a number of laboratories have shown that phase-pure Ni_2P can be prepared on silica only if excess P is used in the oxidic precursor [16,17,20,24]. In our laboratory, for example, silica-supported Ni_2P was prepared from oxidic precursors having $P/Ni \geqslant 0.80$; an oxidic precursor with $P/Ni = 0.50$, the stoichiometric ratio, yielded a mixture of Ni_2P and $Ni_{12}P_5$ on the support [24]. On the other hand, phase-pure Co_2P on silica was prepared from an oxidic precursor that contained the stoichiometric molar ratio, $P/Co = 0.50$ [11]. The $Co_xNi_{2-x}P_y/SiO_2$ catalysts investigated in this work were prepared from oxidic precursors having nominal P/Me molar ratios of 0.50, but a few catalysts having the general composition of $Co_{0.08}Ni_{1.92}P_y/SiO_2$, were prepared from oxidic precursors containing excess P ($0.60 \leqslant P/Me \leqslant 1.1$). For the $Co_xNi_{2-x}P_y/SiO_2$ catalysts prepared from oxidic precursors having a nominal $P/Me = 0.50$, the actual compositions were slightly P-rich, lying in the range $P/Me = 0.53$–0.55, which is similar to that of a Co_2P/SiO_2 catalyst ($P/Co = 0.53$). Not surprisingly, the $Co_xNi_{2-x}P_y/SiO_2$ catalysts prepared from oxidic precursors containing excess P had compositions which were more P-rich. A $Co_{0.08}Ni_{1.92}P_{1.60}/SiO_2$ catalyst had a phosphorus-to-metal ratio of $P/Me = 0.64$, which is similar to the value of $P/Ni = 0.61$ reported previously for a $Ni_{2.00}P_{1.60}/SiO_2$ catalyst [24]. As will be discussed shortly, this excess P in the metal phosphide particles is believed to play an important role in the high activity and stability of these materials for HDS.

Despite having bulk compositions that were P-rich ($P/Me > 0.50$), the surfaces of $Co_{2.00}P_{1.00}/SiO_2$ and $Ni_{2.00}P_{1.60}/SiO_2$ catalysts were metal-rich ($P^s/Me^s < 0.50$), as indicated by the composition data in Table 1. Interestingly, the $Co_xNi_{2-x}P_{1.00}/SiO_2$ catalysts prepared in this study have surfaces that were not only P-rich relative to the expected stoichiometry of the metal phosphide phases (i.e. $P^s/Me^s > 0.50$), but were also P-rich relative to the actual bulk composition of the catalysts with one exception ($Co_{0.04}Ni_{1.96}P_{1.00}/SiO_2$). A $Co_xNi_{2-x}P_y/SiO_2$ catalyst that was prepared from an oxidic precursor containing excess P, $Co_{0.08}Ni_{1.92}P_{1.60}/SiO_2$, had a highly P-enriched surface ($P^s/Me^s = 0.91$) relative to $Ni_{2.00}P_{1.60}/SiO_2$ ($P^s/Me^s = 0.45$). Abu and Smith [32] observed similar surface P-enrichment for unsupported phosphide catalysts having the general formula Co_xNi_2P where $0.08 \leqslant x \leqslant 0.34$. While the catalysts had nominal bulk P/Me molar ratios that were metal-rich ($P/Me < 0.50$), the surfaces of the catalysts were P-rich ($1.2 \leqslant P^s/Me^s \leqslant 4.8$). This is in contrast to the unsupported Ni_2P catalyst investigated, which had a nominal bulk composition of $P/Ni = 0.50$ and a measured surface composition of $P^s/Ni^s = 0.5$. Taken together, the results of Abu et al. [32] and those of the current study indicate that incorporation of relatively small amounts of Co into Ni_2P catalysts leads to surface enrichment of P. We believe that these observations can be understood in terms of the solid state chemistry of the metal phosphide particles. As discussed above, neutron diffraction measurements revealed that there is ordering of the metals in the M(1) and M(2) sites in $Co_xNi_{2-x}P$ materials, with Ni atoms occupying more M(2) sites than M(1) sites. Since Ni atoms in M(2) sites are bonded to five P atoms while Ni atoms in M(1) sites are bonded to four P atoms, a higher proportion of Ni atoms in M(2) sites at the surface of the phosphide particles would lead to more P-rich surfaces.

4.2. HDS properties of $Co_xNi_{2-x}P_y/SiO_2$ catalysts

As briefly summarized in the Introduction, the few studies of bimetallic phosphide catalysts reported in the literature have shown these phosphide materials to have HDS or HDN activities that are lower than, in between, or higher than the catalytic activities of the monometallic phosphides of the same metals. The $Co_xNi_{2-x}P_y/SiO_2$ catalysts investigated in this study show similar variability in their HDS activities relative to those of Co_2P/SiO_2 and

Ni_2P/SiO_2 catalysts, as the activities of the bimetallic phases show a strong dependence on composition. For $Co_xNi_{2-x}P_{1.00}/SiO_2$ catalysts with substantial Co contents ($0.50 < x < 2.00$), the HDS activities were similar to or less than that of Co_2P/SiO_2, while the activities for catalysts with $x \leqslant 0.50$ increased dramatically (as the Co content decreased) and approached that of a $Ni_{2.00}P_{1.60}/SiO_2$ catalyst optimized in an earlier investigation [24]. Since the optimized nickel phosphide catalyst was prepared from an oxidic precursor containing excess P (P/Ni = 0.80), the effect of excess P on HDS activity for the fixed metal composition $Co_{0.08}Ni_{1.92}P_y/SiO_2$ was investigated ($1.00 < y \leqslant 2.20$). Excess P in the oxidic precursors affected the HDS activity strongly, with the catalyst with the optimal composition, $Co_{0.08}Ni_{1.92}P_{2.00}/SiO_2$ (P/Me = 1.00) having an HDS activity that was 34% higher than that of the $Ni_{2.00}P_{1.60}/SiO_2$ catalyst. While the excess P in the $Ni_{2.00}P_{1.60}/SiO_2$ catalyst precursor was necessary to form phase pure Ni_2P on the silica support, no excess P was needed in the $Co_{0.08}Ni_{1.92}P_y/SiO_2$ catalysts to form a phase pure bimetallic phosphide phase on the support. Further addition of P in the oxidic precursor of the Ni_xP_y/SiO_2 catalysts (i.e. P/Ni > 0.80) also resulted in phase pure Ni_2P on the support, but the catalysts HDS activity decreased due to dramatically lower active site densities as measured by O_2 chemisorption. On the other hand, inclusion of excess P up to a molar ratio P/Me = 1.00 in the oxidic precursors of $Co_{0.08}Ni_{1.92}P_y/SiO_2$ catalysts resulted in increased HDS activity; a $Co_{0.08}Ni_{1.92}P_{2.00}/SiO_2$ catalyst was 1.5 times more active than a $Co_{0.08}Ni_{1.92}P_{1.00}/SiO_2$ catalyst. While XPS spectra were not acquired for the $Co_{0.08}Ni_{1.92}P_{2.00}/SiO_2$ catalyst, surface composition results from XPS spectra for a $Co_{0.08}Ni_{1.92}P_{1.60}/SiO_2$ catalyst that was also highly active indicate significant surface P enrichment ($P^s/Me^s = 0.91$) relative to the $Co_{0.08}Ni_{1.92}P_{1.00}/SiO_2$ catalyst ($P^s/Me^s = 0.59$). Despite this high surface P content, the $Co_{0.08}Ni_{1.92}P_{1.60}/SiO_2$ catalyst adsorbed a similar amount of O_2 (118 μmol/g) following an H_2 pretreatment as did the $Co_{0.08}Ni_{1.92}P_{1.00}/SiO_2$ catalyst (127 μmol/g), indicating that the excess P in the bimetal phosphide catalysts was not blocking adsorption sites as was observed previously for Ni_xP_y/SiO_2 catalysts with P/Ni > 0.80. The HDS and surface composition results for the $Co_xNi_{2-x}P_{1.00}/SiO_2$ catalysts indicate that low HDS activities are associated with high surface Co contents and/or low surface P contents, while high HDS activities are associated with high surface P content, and the metal at the surface being Ni. The latter combination is best realized for $Co_xNi_{2-x}P_y/SiO_2$ catalysts containing small amounts of Co ($x \approx 0.08$) and a substantial excess of P ($1.60 \leqslant y \leqslant 2.00$) in the oxidic precursor. Noting the solid state chemistry findings discussed above, we conclude that there is a high density of Ni atoms in M(2) sites at the surfaces of the $Co_{0.08}Ni_{1.92}P_y/SiO_2$ catalysts. As a result, these materials can accommodate substantial excess P, have P-enriched surfaces, and have high HDS activities.

To explore the role of surface P in HDS over phosphide catalysts, Abu and Smith [32] probed the acidity of unsupported Ni_2P and Co_xNi_2P catalysts using *n*-propylamine and correlated their findings with the activities of these catalysts for 4,6-DMDBT HDS. A $Co_{0.08}Ni_2P$ catalyst, which had a highly P-enriched surface (relative to the Ni_2P), adsorbed over three times more *n*-propylamine than did the Ni_2P catalyst. In addition, the $Co_{0.08}Ni_2P$ catalyst was 1.7 times more active for 4,6-DMDBT HDS than Ni_2P on a weight basis and twice as active on a turnover frequency basis. The authors attributed this increased HDS activity to the enhanced acidity of the bimetallic phosphide catalyst due to the enrichment of P at its surface. Based on analysis of the product selectivities, the authors concluded that the higher activity of the $Co_{0.08}Ni_2P$ catalyst relative to Ni_2P was due to significantly enhanced HDS via the direct desulfurization pathway for the bimetallic phosphide catalyst. The higher surface acidity of the $Co_{0.08}Ni_2P$ catalyst may promote migration of methyl groups to give isomerized products such as 2,8-DMDBT, which are more reactive for direct desulfurization than is 4,6-DMDBT. Increased catalyst acidity due to surface enrichment of P on $Co_xNi_{2-x}P_y/SiO_2$ catalysts may also play a role in the thiophene HDS activities measured in the current study, but this was not investigated. However, since thiophene HDS proceeds exclusively via the direct desulfurization pathway on most catalysts and no methyl migration is possible, we expect this factor is less dominant than it might be for 4,6-DMDBT HDS.

Consistent with HDS activity versus time on-stream data reported for Co_2P/SiO_2, CoP/SiO_2 and Ni_2P/SiO_2 catalysts [11,20,24], the $Co_xNi_{2-x}P_y/SiO_2$ catalysts exhibited remarkable stability under HDS conditions with no indication of deactivation during the ~75 h on-stream. Any initial deactivation of the catalysts due to S incorporation likely occurred during the first few turnovers of thiophene on the catalyst sites, which would be too rapid to observe on the time-scale of the sampling (15 min). As discussed in Section 4.3, we conclude that the amount of S incorporation into the catalysts plays an important role in determining the activity of the $Co_xNi_{2-x}P_y/SiO_2$ catalysts.

4.3. Surface chemistry of HDS-tested $Co_xNi_{2-x}P_y/SiO_2$ catalysts

In order to be effective hydrotreating catalysts, candidate materials must possess high activity while also being resistant to sulfur poisoning. A number of studies reported in the literature have shown nickel phosphide catalysts to be highly active and stable HDS catalysts [9,10,14,17–21,24–29,46]. Bulk analyses have revealed remarkably low S incorporation into Ni_xP_y/SiO_2 and Co_xP_y/SiO_2 catalysts after HDS testing or treatment in H_2S/H_2 [11, 21,24,46]. Sawhill et al. [24] measured a bulk particle composition of $Ni_{2.0}P_{1.0}S_{0.017}$ for a 30 wt% Ni_2P/SiO_2 catalyst following H_2S/H_2 at 650 K, which can be compared with a composition of $Ni_{2.0}P_{1.2}S_{0.060}$ determined by Oyama et al. [21] for a 24.4 wt% Ni_2P/SiO_2 catalyst following dibenzothiophene HDS at 643 K. Further, it was observed that the S content of H_2S/H_2-treated or HDS-tested Ni_xP_y/SiO_2 catalysts decreased with increasing bulk P/Ni molar ratio [21,24,46], and as the surface P/Co molar ratio increased for H_2S/H_2-treated Co_xP_y/SiO_2 catalysts [11]. The surface composition of $Ni_{2.87}P_{1.00}S_{0.32}$ measured in the current study for a tested $Ni_{2.00}P_{1.60}/SiO_2$ catalyst can be compared with a surface composition of $Ni_{0.33}P_{1.00}S_{0.04}$ determined by Korányi [14] for a sample of unsupported Ni_2P treated in H_2S/H_2 at 673 K. The lower surface S content measured for the unsupported Ni_2P is likely due to the high surface P/Ni molar ratio for this material relative to the $Ni_{2.00}P_{1.60}/SiO_2$ catalyst. The HDS-tested $Co_xNi_{2-x}P_y/SiO_2$ catalysts had lower surface S contents than either the $Co_{2.00}P_{1.00}/SiO_2$ or $Ni_{2.00}P_{1.60}/SiO_2$ catalysts investigated in this study. Indeed, a $Co_{0.08}Ni_{1.92}P_{1.60}/SiO_2$ catalyst had a surface S content that was just 31% of that of the $Ni_{2.00}P_{1.60}/SiO_2$ catalyst (on an S/Me basis). The resistance of the $Co_xNi_{2-x}P_y/SiO_2$ catalysts to S incorporation can be correlated with the surface P enrichment of these materials relative to the monometallic $Co_{2.00}P_{1.00}/SiO_2$ or $Ni_{2.00}P_{1.60}/SiO_2$ catalysts as indicated by the data plotted in Fig. 6. Additional insight into the surface properties of the $Co_xNi_{2-x}P_y/SiO_2$ catalysts in the sulfiding conditions of an HDS reactor can be gained from the O_2 chemisorption data for the catalysts following H_2 and H_2S/H_2 pretreatments. While the chemisorption capacities of the $Co_{2.00}P_{1.00}/SiO_2$, $Ni_{2.00}P_{1.60}/SiO_2$ and Co-rich $Co_xNi_{2-x}P_y/SiO_2$ catalysts were lower following the H_2S/H_2 pretreatment (relative to the H_2 pretreatment), indicating a loss of active sites, the Ni-rich $Co_xNi_{2-x}P_y/SiO_2$ catalysts had higher chemisorption capacities following the H_2S/H_2 pretreatment. For example, the highly active $Co_{0.08}Ni_{1.92}P_{1.60}/SiO_2$ catalyst had a 35% higher O_2 chemisorption capacity following the H_2S/H_2 pretreatment than after the H_2 pretreatment. Two possible explanations for the higher chemisorption capacities for these Ni-rich $Co_xNi_{2-x}P_y/SiO_2$ catalysts after the

H_2S/H_2 pretreatment are the following: (1) Incorporation of a very small amount of S into the catalysts is beneficial due to formation of a surface phosphosulfide phase, which has a higher site density than the surface phosphide phase that results from reduction in pure H_2. (2) Pretreatment in a H_2S/H_2 mixture may be more effective at removing the passivation layer formed on the phosphide particles after TPR, thus exposing more adsorption sites, than is a similar pretreatment in pure H_2. What is clear is that the small quantity of S incorporated into Ni-rich $Co_xNi_{2-x}P_y/SiO_2$ catalysts during H_2S/H_2 pretreatment (or HDS) does not block a significant number of adsorption sites. Based on the surface composition of the $Co_{0.08}Ni_{1.92}P_{1.60}/SiO_2$ catalyst after HDS testing, $Co_{0.13}Ni_{1.59}P_{1.00}S_{0.06,}$ only 4% of surface Ni atoms would be blocked by S if it is assumed that the sulfur adsorbs exclusively on surface Ni atoms. Assuming that the O_2 chemisorption capacities following H_2S/H_2 pretreatment provide good estimates of the active site densities under HDS conditions, turnover frequencies of 0.017 and 0.019 s^{-1} can be calculated for the $Ni_{2.00}P_{1.60}/SiO_2$ and $Co_{0.08}Ni_{1.92}P_{1.6}/SiO_2$ catalysts, respectively. These values are similar within the uncertainties of the measurements and we conclude, therefore, that the high HDS activity of the $Co_{0.08}Ni_{1.92}P_{1.60}/SiO_2$ catalyst can be traced to its remarkably high site density under the sulfiding conditions present in HDS processing. Consistent with these findings and the solid-state chemistry evidence that suggests that Ni atoms in $Co_xNi_{2-x}P_y/SiO_2$ catalysts occupy disproportionately more pyramidal M(2) sites than tetrahedral M(1) sites, we further conclude that the high site densities of these catalysts are due to Ni atoms in surface M(2) sites, which results in P-enriched surfaces that are resistant to site blockage due to S incorporation.

5. Conclusions

The HDS activities of a series of $Co_xNi_{2-x}P_y/SiO_2$ catalysts have been measured and correlated with the bulk and surface properties of the catalysts. An oxidic precursor composition of $Co_{0.08}Ni_{1.92}P_{2.00}$ on the silica support yielded the bimetallic phosphide phase having the highest HDS activity, 34% higher than that of an optimized nickel phosphide catalyst prepared from an oxidic precursor having a composition of $Ni_{2.00}P_{1.60}$. X-ray photoelectron spectroscopy revealed Ni-rich $Co_xNi_{2-x}P_y/SiO_2$ catalysts (e.g., $Co_{0.08}Ni_{1.92}P_{1.60}$) to have surface enrichment of P relative to monometallic phosphide catalysts (e.g., $Ni_{2.00}P_{1.60}/SiO_2$ and $Co_{2.00}P_{1.00}/SiO_2$) and to incorporate remarkably low amounts of S during HDS testing. The high activities of these $Co_xNi_{2-x}P_y/SiO_2$ catalysts are attributed to surface enrichment of P relative to nickel phosphide, which results in improved resistance to S incorporation under HDS conditions. Consistent with these findings and solid-state chemistry evidence reported by others, we conclude that Ni atoms in Ni-rich $Co_xNi_{2-x}P_y/SiO_2$ catalysts occupy disproportionately more pyramidal M(2) sites than tetrahedral M(1) sites, and that the high site densities of these catalysts are due to Ni atoms in surface M(2) sites, which results in P-enriched surfaces that are resistant to site blockage due to S incorporation.

Acknowledgments

This research was supported by the National Science Foundation under grant number CHE-0503777. A portion (TEM, XPS) of the research described in this paper was performed in the Environmental Molecular Sciences Laboratory (EMSL), a national scientific user facility sponsored by the Department of Energy's Office of Biological and Environmental Research and located at Pacific Northwest National Laboratory. The authors would like to acknowledge Prof. S.T. Oyama for assistance in preparing the crystal structure drawing and helpful discussions.

References

[1] P. Clark, X. Wang, S.T. Oyama, J. Catal. 207 (2002) 256.
[2] D.C. Phillips, S.J. Sawhill, R. Self, M.E. Bussell, J. Catal. 207 (2002) 266.
[3] V. Zuzaniuk, R. Prins, J. Catal. 219 (2003) 85.
[4] A. Montesinos-Castellanos, E. Lima, J.A. de los Reyes, V. Lara, J. Phys. Chem. C 111 (2007) 13898.
[5] A. Montesinos-Castellanos, T.A. Zepeda, B. Pawelec, J.L.G. Fierro, J.A. de los Reyes, Chem. Mater. 19 (2007) 5627.
[6] A. Montesinos-Castellanos, T.A. Zepeda, B. Pawelec, E. Lima, J.L.G. Fierro, A. Olivas, J.A. de los Reyes, Appl. Catal. A Gen. 334 (2008) 330.
[7] P. Clark, W. Li, S.T. Oyama, J. Catal. 200 (2001) 140.
[8] S.T. Oyama, P. Clark, X. Wang, T. Shido, Y. Iwasawa, S. Hayashi, J.M. Ramallo-Lopez, F.G. Requejo, J. Phys. Chem. B 106 (2002) 1913.
[9] X. Wang, P. Clark, S.T. Oyama, J. Catal. 208 (2002) 321.
[10] S.T. Oyama, J. Catal. 216 (2003) 343.
[11] A.W. Burns, K.A. Layman, D.H. Bale, M.E. Bussell, Appl. Catal. A Gen. 343 (2008) 68.
[12] W.R.A.M. Robinson, J.N.M. van Gestel, J. Catal. 161 (1996) 539.
[13] V. Zuzaniuk, C. Stinner, R. Prins, T. Weber, Stud. Surf. Sci. Catal. 143 (2002) 247.
[14] T. Korányi, Appl. Catal. A Gen. 239 (2003) 253.
[15] C. Stinner, R. Prins, T. Weber, J. Catal. 202 (2001) 187.
[16] C. Stinner, Z. Tang, M. Haouas, T. Weber, R. Prins, J. Catal. 208 (2002) 456.
[17] S.T. Oyama, X. Wang, Y.-K. Lee, K. Bando, F.G. Requejo, J. Catal. 210 (2002) 207.
[18] S.T. Oyama, X. Wang, F.G. Requejo, T. Sato, Y. Yoshimura, J. Catal. 209 (2002) 1.
[19] J.A. Rodriguez, J.-Y. Kim, J.C. Hanson, S.J. Sawhill, M.E. Bussell, J. Phys. Chem. B 107 (2003) 6276.
[20] S.J. Sawhill, D.C. Phillips, M.E. Bussell, J. Catal. 215 (2003) 208.
[21] S.T. Oyama, X. Wang, Y.-K. Lee, W.-J. Chun, J. Catal. 221 (2004) 263.
[22] K.A. Layman, M.E. Bussell, J. Phys. Chem. B 108 (2004) 10930.
[23] K.A. Layman, M.E. Bussell, J. Phys. Chem. B 108 (2004) 15791.
[24] S.J. Sawhill, K.A. Layman, D.R. Van Wyk, M.H. Engelhard, C. Wang, M.E. Bussell, J. Catal. 231 (2005) 300.
[25] Y.-K. Lee, S.T. Oyama, J. Catal. 239 (2006) 376.
[26] M. Lu, A. Wang, X. Li, M. Zhang, K. Tao, Energy Fuels 21 (2007) 554.
[27] Y.-K. Lee, Y. Shu, S.T. Oyama, Appl. Catal. A Gen. 322 (2007) 191.
[28] I.I. Abu, K.J. Smith, Appl. Catal. A Gen. 328 (2007) 58.
[29] T. Koranyi, Z. Vit, C.C. Poduval, R. Ryoo, H.S. Kim, E.J.M. Hensen, J. Catal. 253 (2008) 119.
[30] I.I. Abu, K.J. Smith, Catal. Today 125 (2007) 248.
[31] F. Sun, W. Wu, Z. Wu, J. Guo, Z. Wei, Y. Yang, Z. Jiang, F. Tian, C. Li, J. Catal. 228 (2004) 298.
[32] I.A. Abu, K.J. Smith, J. Catal. 241 (2006) 356.
[33] D. Ma, T. Xiao, S. Xie, W. Zhou, S.L. Gonzalez-Cortes, M.L.H. Green, Chem. Mater. 16 (2004) 2697.
[34] J.P. Sénateur, A. Rouault, P. L'Héritier, A. Krumbügel-Nylund, R. Fruchart, Mater. Res. Bull. 8 (1973) 229.
[35] JCPDS Powder Diffraction File, International Centre for Diffraction Data, Swarthmore, PA, 2000.
[36] D. Briggs, M.P. Seah (Eds.), Practical Surface Analysis by Auger and X-Ray Photoelectron Spectroscopy, Wiley, New York, 1983.
[37] V.V. Nemoshalenko, V.V. Didyk, V.P. Krivitskii, A.I. Senekevich, Zh. Neorg. Khim. 28 (1983) 2182.
[38] H. Hou, Q. Peng, S. Zhang, Q. Guo, Y. Xie, Eur. J. Inorg. Chem. (2005) 2625.
[39] F. Hulliger, Struct. Bond. (Berlin) 4 (1968) 83.
[40] R. Fruchart, A. Roger, J.P. Senateur, J. Appl. Phys. 40 (1969) 1250.
[41] J.B. Goodenough, J. Solid State Chem. 7 (1973) 428.
[42] M. Artigas, M. Bacmann, D. Boursier, D. Fruchart, R. Fruchart, J.L. Soubeyroux, C.R. Acad. Sci. Paris Ser. II 315 (1992) 29.
[43] Y. Maeda, Y. Takashima, J. Inorg. Nucl. Chem. 35 (1973) 1963.
[44] Unpublished results.
[45] S.T. Oyama, Y.-K. Lee, J. Catal. 258 (2008) 393.
[46] Y. Shu, Y.-K. Lee, S.T. Oyama, J. Catal. 236 (2005) 112.